Molecular Pharmacology Fast Forward. Published on March 26, 2015 as DOI: 10.1124/mol.114.094987
This article has not been copyedited and formatted. The final version may differ from this version.

TITLE PAGE

Title: The Novel Ribonucleotide Reductase Inhibitor COH29 Inhibits DNA Repair In Vitro.

Authors: Mei-Chuan Chen, Bingsen Zhou, Keqiang Zhang, Yate-Ching Yuan, Frank Un, Shuya Hu, Chih-Ming Chou, Chun-Han Chen, Jun Wu, Yan Wang, Xiyong Liu, D. Lynne Smith, Hongzhi Li, Zheng Liu, Charles D. Warden, Leila Su, Linda H. Malkas, Young Min Chung, Mickey C-T Hu, and Yun Yen

Affiliations: City of Hope National Medical Center, 1500 East Duarte Road, Duarte, CA 91010 USA: Department of Molecular Pharmacology; BZ, FU, SH, XL, DLS, KZ, YY: Department of Molecular Medicine; Y-CY, HL, ZL, CDW, LS: Department of Molecular and Cellular Biology; LHM: Division of Comparative Medicine; JW, YW.

Stanford University School of Medicine, Stanford, CA 94305 USA: Division of Gynecologic Oncology, Department of Obstetrics and Gynecology, YMC, MC-TH

Taipei Medical University, 250 Wu-Hsing Street, Taipei 110, Taiwan: Ph.D. Program for the Clinical Drug Discovery from Botanical Herbs and Graduate Institute of Pharmacognosy, College of Pharmacy, M-CC; Ph.D. Program for Cancer Biology and Drug Discovery, College of Medical Science and Technology, CHC, YY; ,Department of Biochemistry, School of Medicine, College of Medicine, C-MC

Molecular Pharmacology Fast Forward. Published on March 26, 2015 as DOI: 10.1124/mol.114.094987
This article has not been copyedited and formatted. The final version may differ from this version.

RUNNING TITLE PAGE

Running title: RNR inhibitor COH29 interferes with DNA repair pathways

Corresponding Author: Yun Yen

Professor, Ph.D Program for Cancer Biology and Drug Discovery, Taipei Medical University

250 Wuxing Street, Taipei 11031, Taiwan

Tel: +886-2-2736-6485

Fax: +886-2-2378-7795

E-mail: yyen@tmu.edu.tw

Number of text pages: **19**

Number of tables: **2**

Number of figures: **6**

Number of references: **33**

Abstract word count: **232**

Introduction word count: **646**

Discussion word count: **887**

Non-standard abbreviations: 3-AP, 3-aminopyridine-2-carboxaldehyde thiosemicarbazone; ATM, ataxia-telangiectasia-mutated; ATM and Rad 3-related; BER, base-excision repair; BRCA-1, breast cancer associated gene 1; Chk1, checkpoint kinase 1; Chk2, checkpoint kinase 2; COH29, N-(4-(3,4-dihydroxyphenyl)-5-phenylthiazol-2-yl)-3,4-dihydroxybenzamide; cRNA, complementary RNA; DDR, DNA-

Molecular Pharmacology Fast Forward. Published on March 26, 2015 as DOI: 10.1124/mol.114.094987
This article has not been copyedited and formatted. The final version may differ from this version.

damage response; dpf, days post-fertilization; DSB, double strand breaks; GFP, green fluorescence protein; hpf, hours post-fertilization; HR, homologous recombination; HU, hydroxyurea; MTT, 3-(4,5-Dimethylthiazol-2-yl)-2,5-diphenyltetrazolium bromide; NER, nucleotide-excision repair; NHEJ, nonhomologous end joining; NSG, NOD scid gamma; RNR, ribonucleotide reductase; RT-PCR, reverse transcription polymerase chain reaction; siRNA, small interfering RNA; SSBR, single strand DNA break repair; wt, wild-type; γ-H2AX, gamma H2A histone family member X.

Molecular Pharmacology Fast Forward. Published on March 26, 2015 as DOI: 10.1124/mol.114.094987
This article has not been copyedited and formatted. The final version may differ from this version.

ABSTRACT

COH29, a novel antimetabolite drug developed at City of Hope Cancer Center, has anticancer activity that stems primarily from the inhibition of human ribonucleotide reductase (RNR). This key enzyme in deoxyribonucleotide biosynthesis is the target of established clinical agents such as hydroxyurea (HU) and gemcitabine because of its critical role in DNA replication and repair. Herein we report that BRCA-1-defective human breast cancer cells are more sensitive than wild-type BRCA-1 counterparts to COH29 *in vitro* and *in vivo*. Microarray gene expression profiling showed that COH29 reduces expression of DNA repair pathway genes, suggesting that COH29 interferes with these pathways. It is well-established that BRCA1 plays a role in DNA damage repair, especially homologous recombination (HR) repair, to maintain genome integrity. In BRCA1-defective HCC1937 breast cancer cells, COH29 induced more double-strand breaks (DSB) and DNA-damage response (DDR) than in HCC1937+BRCA1 cells. By EJ5- and DR-GFP reporter assay, we found COH29 could inhibit NHEJ efficiency and that no HR activity was detected in HCC1937 cells, suggesting the repression of the NHEJ repair pathway may be involved in COH29-induced DSB in BRCA1-deficient HCC1937 cells. Furthermore, we observed accumulation of nuclear Rad51 foci in COH29-treated HCC1937+BRCA1 cells, suggesting BRCA1 plays a crucial role in repairing/recovering drug-induced DNA damage by recruiting Rad51 to damage sites. In summary, we have described additional biological effects of the RNR inhibitor COH29 that potentially strengthen its utility as an anticancer agent.

Molecular Pharmacology Fast Forward. Published on March 26, 2015 as DOI: 10.1124/mol.114.094987
This article has not been copyedited and formatted. The final version may differ from this version.

INTRODUCTION

The prototypic antimetabolite drug hydroxyurea (HU) has been used to treat a variety of human cancers including chronic myelogenous leukemia, head and neck cancer, and others (Hehlmann 2003, Shewach and Lawrence 2007). Its primary anticancer and cellular target is ribonucleotide reductase (RNR), which reduces ribonucleotides to their corresponding deoxy forms to supply dNTPs for DNA replication and repair (Reichard and Ehrenberg 1983, Xue et al. 2003). The human RNR is composed of the hRRM1 and hRRM2 subunits (Reichard and Ehrenberg 1983, Xue et al. 2003). Following a genotoxic stimulus, an alternate RNR enzyme, which is composed of hRRM1 and p53R2 (a homologue of hRRM2 transactivated by the tumor suppressor protein p53) is induced to supply dNTPs for DNA repair (Shao et al. 2004). Within cells, HU inhibits both types of RNR (Shao et al. 2004) through generating free radicals via oxidative transformation (Young and Hodas 1964) that quenches free-radical mediated catalysis (Reichard and Ehrenberg 1983). Blocking this signaling can arrest DNA replication and reduce cell growth (Shewach and Lawrence 2007). However, therapeutically, HU is limited by its short half-life and problematic side effects, most notably myelosuppression, and gastrointestinal and dermatologic effects (Platt 2008).

COH29 is an RNR inhibitor that demonstrates promise as an anti-cancer agent and is currently in preclinical development at City of Hope Cancer Center. COH29 is an aromatically substituted thiazole compound that occupies a structurally conserved ligand-binding pocket on the hRRM2 subunit located at the hRRM1/hRRM2 interface, thereby inhibiting hRRM1/hRRM2 assembly, effectively inhibiting RR activity (Zhou et al. 2013). *In vitro* COH29 inhibits the proliferation of multiple human cancer cell lines with an IC_{50} less than 10 μM in most cases. Treatment of cancer cells with COH29 led

Molecular Pharmacology Fast Forward. Published on March 26, 2015 as DOI: 10.1124/mol.114.094987
This article has not been copyedited and formatted. The final version may differ from this version.

to a dose-dependent S-phase arrest, induction of apoptosis, and cell death (Zhou et al. 2013). One major advantage of COH-29 over other RR inhibitors in development, such as 3-aminopyridine-2-carboxaldehyde thiosemicarbazone (triapine, 3-AP), is that it does not appear to be an iron chelator, reducing the potential side effects.

In response to DNA damage numerous DNA-repair pathway proteins collectively act to restore DNA continuity and genomic integrity (Helleday et al. 2008). Among these different repair pathways, base-excision repair (BER) and nucleotide-excision repair (NER) are both involved in the removal of lesions and their replacement with short stretches of DNA. The continuing presence of single strand breaks during DNA replication will lead to stalled replication forks, whose resolution recombination (HR) or non-homologous end joining (NHEJ) repair which is responsible for DNA DSBs (double-strand breaks) (Moeller et al. 2009, Gottipati et al. 2010). The biochemical processes of HR are mediated by multiple conserved factors including the essential recombinase RAD51, tumor suppressors BRCA1, and BRCA2 (Curtin 2012).

The efficacy of DNA-damaging drugs is highly influenced and modulated by cellular DNA repair capacity (Helleday et al. 2008). Indeed, small-molecule inhibitors of DNA repair have been combined with conventional chemotherapy drugs in preclinical studies (Miknyoczki et al. 2003), indicating that the DNA repair machinery is a promising target for novel cancer treatments.

Herein we report that COH29 exhibits enhanced cytotoxicity in BRCA1-deficient HCC1937 cells compared with HCC1937+BRCA1 cells accompanied by significant DNA DSB marker (γH2AX) accumulation in the BRCA1-defective cells, suggesting BRCA1 prevents prolonged presence of DSBs. In addition, we also found that COH29 reduced

Molecular Pharmacology Fast Forward. Published on March 26, 2015 as DOI: 10.1124/mol.114.094987
This article has not been copyedited and formatted. The final version may differ from this version.

NHEJ repair efficiency in a concentration-dependent manner. In the setting of the BRCA1-defective HCC1937 cells, which we also show are HR-deficient, this inhibition of NHEJ by COH29 dramatically reduced repair of DNA lesions. Indicative of this is that after COH29 treatment fewer Rad51 nuclear foci were observed in HCC1937 than in HCC1937+BRCA1 cells. In addition, our microarray results revealed that COH29 downregulated various DNA repair genes. These data suggest defective HR and NHEJ DNA repair pathways may contribute to the cytotoxicity of COH29 in BRCA1-deficient cells, and as a corollary that BRCA1 status plays a central role in determining the cytotoxicity of COH29 in cancer cells.

Molecular Pharmacology Fast Forward. Published on March 26, 2015 as DOI: 10.1124/mol.114.094987
This article has not been copyedited and formatted. The final version may differ from this version.

MATERIALS & METHODS

Cell lines

All cell lines were acquired from the American Type Culture Collection (Manassas, VA, USA), and were maintained in RPMI 1640 medium (Mediatech) with 10% fetal bovine serum, 2 mM glutamine, and 100 U of penicillin and 100 µg of streptomycin per ml of medium (Sigma) at 37^{o}C in 5% CO_2. To isolate HCC1937+BRCA1 cells, parental HCC1937 cells were transfected with pcDNA3.1 plasmid expressing full-length BRCA1 cDNA. Stable transfectant clones were selected and used for drug sensitivity assays. For stable transfection, cells at 30-40% confluence were incubated overnight with 2 µg of plasmid DNA, using FuGENE 6 transfectin reagent (Roche Molecular Biochemical, Monza, Italy) according to the manufacturer's instructions. Cells were then selected in puromycin (1 µg/ml) (Invitrogen Life Technologies, La Jolla, CA, USA). After 20 to 30 days, viable puromycin-resistant colonies from HCC1937 transfections were expanded and screened. The clones that stably expressed puromycin and retained growth potential were assayed for BRCA1 expression by Western blot analysis. By Western blot analysis, we evaluated the restoration of BRCA1 expression in the puromycin-resistant cDNA/transfectant cells. These transfected cells showed an increased expression of BRCA1 protein, suggesting effective restoration of protein expression.

Reagents

COH29 (N-(4-(3,4-dihydroxyphenyl)-5-phenylthiazol-2-yl)-3,4-dihydroxybenzamide) was synthesized and purified at City of Hope. All other recombinant proteins and antibodies were obtained from commercial sources: γH2AX, Cell Signaling Technology (Danvers,

Molecular Pharmacology Fast Forward. Published on March 26, 2015 as DOI: 10.1124/mol.114.094987
This article has not been copyedited and formatted. The final version may differ from this version.

MA, USA); Rad51, Novus (Littleton, CO, USA); beta-actin, Millipore (Billerica, MA, USA); Antibodies specific to FOXO3 (H-144 and N-16, 1:1000), phospho-H2AX serine-139 (γ-H2AX, 1:1,000), Rad51 (1: 1000), β-tubulin (1:1000), Lamin A/C (1:2000 dilution) PARP, and anti-mouse, and anti-rabbit IgGs were obtained from Santa Cruz Biotechnology (Santa Cruz, CA, USA). Antibodies against FOXO3 (1:1,000) and phospho-ATM serine-1981 (ATM-pS1981, 1:1,000 dilution) were obtained from Epitomics (Burlingame, CA) and Millipore (Billerica, MA), respectively. An antibody against p53-pS15 was purchased from Cell Signaling Technology. An anti-p27Kip1 antibody was purchased from BD PharMingen (San Diego, CA). Alexa 488 (green)- and Alexa 594 (red)-conjugated secondary antibodies were obtained from Molecular Probes (Eugene, OR). Anti-Rabbit IgG (whole molecule)–FITC antibody was purchased from Sigma (St. Louis, MO, USA). Rhodamine Red™-X Goat Anti-Mouse IgG was purchased from Invitrogen (Carlsbad, CA, USA).

Immunofluorescence

Immunofluorescence experiments on HCC1937 and HCC1937+BRCA1 cells were conducted as described previously (Chung et al. 2012, Hu et al. 2014). Briefly, cells were grown on glass coverslips. After treatment with COH29 (10 μM) for 24 hours, cells were fixed with 4 % paraformaldehyde for 10 min and permeabilized with Triton X-100 (0.5%). The coverslips were washed with phosphate-buffered saline (PBS) and blocked with PBS-containing 2% bovine serum albumin (BSA), incubated with an antibody specific to FOXO3 or ATM-pS1981 or γ-H2AX or Rad51 (1:50–1:200 dilution), followed by Alexa 488-conjugated anti-rabbit or anti-mouse (1:200), Alexa 594-conjugated anti-

Molecular Pharmacology Fast Forward. Published on March 26, 2015 as DOI: 10.1124/mol.114.094987
This article has not been copyedited and formatted. The final version may differ from this version.

goat (1:100) secondary antibodies (Molecular Probes). Cells were incubated with 4',6-diamidino-2-phenylindole (DAPI; Sigma) to stain the nuclei. Specific staining was visualized and images were captured with a Leica SP2 AOBS confocal laser scanning microscope. To measure foci-positive cells, we used ~300 cells randomly captured by confocal microscopy. The percentages of considering foci-positive cells were calculated from cells containing at least five foci. Each error bar presented is the mean of standard deviation.

Subcellular Fractionation and Immunoblotting

For details of the subcellular fractionation, cells were trypsinized and washed with cold PBS solution twice. After centrifugation at 1,200*g* for 5 min, cells were incubated in buffer (50 mM HEPES, pH 7.5, 150 mM NaCl, 1 mM EDTA) containing 0.2% Nonidet P-40 (NP-40), supplemented with protease inhibitors (5 μg/ml each of pepstatin, leupeptin, and aprotinin) and phosphatase inhibitors on ice for 5 min. Following centrifugation at 1,000*g* for 5 min, the supernatant was collected (i.e., cytoplasmic fraction) and pellets were washed with the same buffer twice. The washed samples were extracted for 40 min on ice with fractionation buffer containing 0.5% NP-40 for nuclear fraction. All the samples were sonicated and clarified by centrifugation at 16,000*g* for 15 min. Protein concentrations of all fractions were determined with Bio-Rad Protein Assay (Bio-Rad Laboratories, Hercules, CA). Immunoblotting was performed as described previously (Chung et al. 2012, Hu et al. 2014).

Cytotoxicity and Viability Assays

Molecular Pharmacology Fast Forward. Published on March 26, 2015 as DOI: 10.1124/mol.114.094987
This article has not been copyedited and formatted. The final version may differ from this version.

Cells were seeded into 96-well plates in 100 µl of complete medium at 2,000 to 5,000 cells per well, depending on cell line growth rate. After overnight incubation, test compound was added to each well at various concentrations in 50 µl of culture medium. After a further incubation for 96 hours at 37ºC, FDA (fluorescein diacetate; final concentration: 10 mg/mL) and eosin Y [final concentration: 0.1% (w/v)] were added to each well and the cells were incubated for an additional 20 minutes at 37 ºC. Cytotoxicity was assessed by Digital Imaging Microscopy System (DIMSCAN) detection (Keshelava et al. 2005).

Viability was assessed using MTS [(3-(4,5-dimethylthiazol-2-yl)-5-(3-carboxymethoxyphenyl)-2-(4-sulfophenyl)-2H-tetrazolium)] as previously described. (Zhou et al. 2013)

Orthotopic Tumor Model

Experiments in mice were conducted under a protocol approved by the IACUC of City of Hope. Female NOD scid gamma (NSG) mice with HCC1937 and HCC1937+BRCA1 cells implanted into the mammary fat pads around the inguinal area were administered 400 mg/kg COH29 in 30% solutol (BASF North America) or vehicle by daily gavage for 28 days. Because HCC1937 and HCC1937+BRCA1 cells form slow-growing tumors, they were implanted using Matrigel™ (Becton-Dickinson Biosciences). To establish tumors 4 x 10^6 cells in 200 µl serum-free medium containing 50% Matrigel™ were injected into the mammary fat pads around the inguinal area of a pair of 8 week old female NSG mice. Once the initial tumors reached 13 mm in diameter, they were dissected out, minced into 3 mm pieces and implanted into the inguinal area of the

Molecular Pharmacology Fast Forward. Published on March 26, 2015 as DOI: 10.1124/mol.114.094987
This article has not been copyedited and formatted. The final version may differ from this version.

mammary fat pads of the experimental mice. When the transplanted tumors reached approximately 50 mm^2, drug treatment was initiated. Tumor diameters were measured by digital calipers over a 28-day period, and the tumor volume calculated using the formula $0.5 \times width^2 \times length$ for each time point. Mice were euthanized once the tumors reached approximately 500 mm^3 in compliance with City of Hope's IACUC stopping rules. Students' t-test was used to determine the statistical significance between COH29 treatment and corresponding vehicle control. The *p* value less than 0.05 (2 sides) was considered to indicate statistical significance.

DNA repair assays

Reporter cell lines for GFP-based DNA damage repair assays were established by stable transfection of HCC1937 and HCC1937+BRCA1 cells with the pimEJ5GFP reporter plasmid for NHEJ (Bennardo et al. 2008) and the pHPRT-DRGFP reporter plasmid for HR (Pierce et al. 2001) respectively, and selected with 0.3 μg/ml puromycin. The resultant HCC1937-EJ5GFP and HCC1937+BRCA1-DRGFP cells were first pretreated with COH29 for 24h, and then transiently transfected with a predetermined mixture of pCBA-SceI plasmid to express I-SceI endonuclease and a plasmid to express DsRed (RFP) protein which served as the control for transfection efficiency. After incubation with COH29 for another 48 h, 5 x 10^5 cells per transfection were analyzed by FACS to count total GFP and DsRed protein positive cells. Each assay was performed three times, and data presented as the ratio of GFP-positive to DsRed-positive cells among whole cells.

siRNA interference assay

Molecular Pharmacology Fast Forward. Published on March 26, 2015 as DOI: 10.1124/mol.114.094987
This article has not been copyedited and formatted. The final version may differ from this version.

The construction of the anti-human BRCA1 siRNA-expressing plasmid was performed as described (Un et al. 2006) using previously published anti-human BRCA1 siRNA sequences (5'-UCACAGUGUCCUUUAUGUA-3" and 5'-UACAUAAAGGACACUGUGA-3'). In each case, the annealed oligonucleotide duplex encoding the siRNA was subcloned into the expression vector psiRNA-hH1zeo (InvivoGen, San Diego, CA, USA) to express under the control of the RNA polymerase III-dependent H1 RNA promoter. Cells were transfected with the indicated plasmid at equimolar concentration via electroporation.

Zebrafish genotoxicity assay

Zebrafish (*Danio rerio*) were obtained from zebrafish Core facility of Taipei Medical University and maintained at 28^{o}C on a 14h light/10h dark cycle. Embryos were incubated at 28^{o}C and different developmental stages were determined as described (Westerfield 1993). Fifteen wild-type embryos each were treated with concentrations of HU (0, 5, 10, 20, 50 mM) or COH29 (0, 10, 20, 50, 100 μM) at 20 hpf (hours post-fertilization) to evaluate the mutagenic effect. Treated embryos were observed at 2, 3, 4, 5 and 6 dpf (days post-fertilization). At 6 dpf, the percentage of fish exhibiting developmental abnormalities and the survival rate was determined. Embryos were observed using an Olympus IX70-FLA inverted fluorescence microscope. Images were taken using SPOT digital camera system (Diagnostic Instruments, Sterling Heights, Michigan, USA) and assembled with *ImageJ* software (Schneider et al. 2012).

Microarray Analysis

Molecular Pharmacology Fast Forward. Published on March 26, 2015 as DOI: 10.1124/mol.114.094987
This article has not been copyedited and formatted. The final version may differ from this version.

For microarray analysis HCC1937 and HCC1937+BRCA1 cells were treated with 10 μM COH29 or vehicle (DMSO) for 24 h. Total RNA was extracted using TRIzol reagent (Invitrogen). Synthesis and labeling of complementary RNA (cRNA) targets, hybridization of GeneChips, and signal detection were carried out by the Integrated Genomics Core Facility at City of Hope. The Affymetrix Human Gene 1.0 ST Array (Affymetrix) was used for microarray gene expression profiles. The microarray was carried out using Ambion's WT Expression kit (Life Technologies) and Affymetrix's GeneChip Terminal labeling system. Briefly, 100 ng of total RNA was used to start the first strand cDNA synthesis using an engineered random primer plus polyT7 promoter. After the second strand cDNA synthesis, the antisense cRNA (in vitro transcription) was generated using T7 RNA polymerase. Then 10 μg of cRNA was used to start the second cycle of cDNA synthesis using random primers plus dUTP and dNTP. The single-strand cDNA was fragmented and then end-labeled with biotinylated nucleotides in the presence of terminal deoxynucleotidyl transferase (TdT) using Affymetrix's WT Terminal Labeling kit. Labeled single-stranded cDNA (5 μg) was hybridized with an Affymetrix Human Gene 1.0 ST array, and the array was scanned using an Affymetrix GeneChip Scanner 3000 7G. Data has been deposited into NCBI Gene Expression Omnibus (GEO) [GSE55004].

Statistical processing of microarray data

Microarray samples were RMA normalized (Irizarry et al. 2003) using Partek® Genomics Suite™ (Version 6.6; Partek, Inc.), and genes were defined as differentially expressed if they showed at least a 1.2 fold-change and false discovery rate (FDR) < 0.05. FDR

Molecular Pharmacology Fast Forward. Published on March 26, 2015 as DOI: 10.1124/mol.114.094987
This article has not been copyedited and formatted. The final version may differ from this version.

values were calculated using the method of Benjamini and Hochberg (Benjamini and Hochberg 1995) from the distribution of ANOVA with Linear Contrast *p*-values. Gene ontology (GO)(Ashburner et al. 2000) enrichment analysis was performed within Partek® Genomics Suite™, and GO categories were defined significant with a Fisher Exact test p-value < 0.05.

Molecular Pharmacology Fast Forward. Published on March 26, 2015 as DOI: 10.1124/mol.114.094987
This article has not been copyedited and formatted. The final version may differ from this version.

RESULTS

COH29 targets BRCA1-defective human cancer cells

Our previous data showed the broad antitumor activity of COH29 in the NCI-60 cell line panel, and that multiple human breast cancer cell lines as well as human ovarian cancer cell lines are sensitive to COH29 (Zhou et al. 2013). Breast and ovarian cancers occur with a greater frequency in carriers of a mutant BRCA1 gene than the general population (Wooster and Weber 2003). We therefore investigated the activity of COH29 in several cell lines with differing BRCA1 status, including OV90 (BRCA1 wild-type), UWB1.289 (BRCA1-mutant), HCC1937 (BRCA1-mutant) and HCC1937+BRCA1 cells. As shown in Fig. 1A, the UWB1.289 ovarian cancer cell line, which expresses truncated BRCA1 protein due to the homozygous 2594delC mutation (DelloRusso et al. 2007), was more sensitive to COH29 (IC_{50}: 12.30±1.15 μM) than the OV90 human ovarian cancer cell line that expresses wild-type BRCA1 (IC_{50}: 31.57±3.35 μM). We further stably expressed BRCA1 in UWB1.289 ovarian cancer cells, which resulted in a more resistant phenotype in response to COH29 treatment compared with the parental UWB1.289 cells (Fig.1B). Likewise, similar results were observed in an isogenic pair of human breast cancer cell lines. HCC1937 cells were more sensitive to COH29 than their BRCA1 wild type expressing counterpart (HCC1937+BRCA1; Fig. 2A). The sensitivity of BRCA1-deficient cells to COH29 was further tested in an orthotopic tumor explant model. The growth of HCC1937 tumors implanted into mouse mammary fat pads was significantly (47.0% $p = 0.0007$) suppressed by daily oral dosing with 400 mg/kg COH29 compared to vehicle by day 28 (Fig. 2B). In contrast, growth of

Molecular Pharmacology Fast Forward. Published on March 26, 2015 as DOI: 10.1124/mol.114.094987
This article has not been copyedited and formatted. The final version may differ from this version.

tumors established with the isogenic HCC1937+BRCA1 cells in COH29-treated mice was not significantly different than in vehicle controls at the same time point (34.3% p = 0.1577; Fig. 2C). As the HCC1937+BRCA1 bearing animals were sacrificed per institutional guidelines at this time, no further comparisons between the effect of COH29 on the growth of the HCC1937 deficient xenografts and HCC1937+BRCA xenografts could be made. However, the HCC1937 xenografts were continued for a total of 60 days, in which the suppression of tumor growth by COH29 continued (data not shown). The *in vitro* data indicated COH29 is more potent in BRCA1-defective cells. Among the IC_{50} values shown in Table 1, COH29 showed 4.8 times more potency in HCC1937 cells compared to HCC1937+BRCA1. Therefore we used these two cell lines in the subsequent experiments to investigate the cause of the differential sensitivity to COH29.

Effect of COH29 on DNA damage checkpoints

Next, we evaluated the effect of COH29 on DNA damage signaling in HCC1937 and HCC1937+BRCA1 cells. COH29 induced significant phosphorylation of checkpoint kinase proteins Chk1, Chk2, and increased the level of the DSB marker γ-H2AX in both cell lines (Fig. 3A). Notably, COH29 triggered more obvious signaling in HCC1937 cells compared with HCC1937+BRCA1 cells in the same concentration range. A similar effect was also detected with HU treatment (Fig. 3B). It has been reported that foxo3 is necessary for ATM-mediated apoptotic signaling after DNA damage (Chung et al. 2012). As shown in Fig. 4A, induction of accumulation of p-ATM, γH2AX, foxo3, and its target protein p27 in the nucleus in response to COH29 was also observed. Furthermore, we found that γH2AX and phospho-ATM colocalize with foxo3 in the nucleus by confocal

Molecular Pharmacology Fast Forward. Published on March 26, 2015 as DOI: 10.1124/mol.114.094987
This article has not been copyedited and formatted. The final version may differ from this version.

immunofluorescence microscopy (Fig. 4B and 4C). These data suggest COH29 activates DNA damage signaling and recruitment of activated-ATM and foxo3 at DNA damage sites.

Differential gene expression in COH29 treated BRCA1-defective human breast cancer cells

We next performed genome-wide microarray analysis using the Affymetrix GeneChip microarray platform to identify the gene expression profiles and pathways affected by COH29 treatment. The RNA expression profile of COH29 treated HCC1937 breast cancer cells lacking BRCA1 was compared with that of COH29 treated HCC1937+BRCA1 cells. Both HCC1937 and HCC1937+BRCA1 cells showed Gene Ontology (GO) enrichment for DNA repair genes (Table 2; *p*-values ranging from 0.0046 – 0.0069) after exposure to 10 μM COH29 for 24 h. These data suggest COH29 may interfere with several DNA repair pathways. This enrichment remained significant for the various subsets of DNA repair genes, including DNA ligation involved in DNA repair, but not HR repair genes when COH29 treated HCC1937 and HCC1937-BRCA1 cells were compared. This is consistent with what we observed in the NHEJ and HR repair reporter assays below.

Effect of COH29 on DNA double-strand breaks (DSBs) repair

DSBs can be repaired either by the homologous recombination (HR) or nonhomologous end joining (NHEJ) pathways. Previous studies have shown that the EJ5- and DR-GFP reporter assays could be used to measure the ability of NHEJ and HR repair

Molecular Pharmacology Fast Forward. Published on March 26, 2015 as DOI: 10.1124/mol.114.094987
This article has not been copyedited and formatted. The final version may differ from this version.

respectively (Bennardo et al. 2008). We next sought to elucidate the role of COH29 in DSB DNA repair, using integrated EJ5-GFP and DR-GFP reporters in HCC1937 cells. In this system transient expression of I-SceI induces DSBs, which if repaired results in the generation of GFP+ cells. GFP signal was hardly detected in HCC1937-DR-GFP cells, while RFP signal indicated successful transfection (Fig. 5B), consistent with the role of BRCA1 as an essential component of HR repair, and indicating HR-deficiency in BRCA1-mutant HCC1937 cells. In addition, we found COH29 suppressed NHEJ repair efficiency in a concentration-dependent manner as shown by reduction in the percentage of GFP + cells in HCC1937-EJ5-GFP assay (Fig. 5B). These data suggest that the COH29-suppressed NHEJ repair pathway may also contribute to the accumulation of DSBs in HR-deficient HCC1937 cells. Recruitment of Rad51 protein at lesions is a well-documented step in the HR repair process to facilitate DNA damage repair (Deng and Brodie 2000). Indeed, we detected obvious Rad51 foci formation in the nucleus in COH29-treated HCC1937/BRCA1 cells compared with COH29-treated HCC1937 cells (Fig. 5C). Similar effects were also observed in HU-treated cells. Taken together, these data further support our hypothesis that BRCA1 may be the key player in determining the sensitivity of cancer cells to COH29.

Genotoxicity of COH29 in embryos of zebrafish

We next assessed the genotoxic effect of COH29 in wild-type zebrafish embryos treated from 1 to 7 dpf (day post-fertilization) with a range of doses of COH29 (0-100 μM). HU (0-50 mM) was included as a positive control because it is known to cause developmental defects. As expected, HU caused defects in eyes and heart by 4 dpf

Molecular Pharmacology Fast Forward. Published on March 26, 2015 as DOI: 10.1124/mol.114.094987
This article has not been copyedited and formatted. The final version may differ from this version.

(Fig. 6A) and resulted in a dose-dependent increase in the number of mutant embryos (Fig. 6B). It is noteworthy that no developmental defects (Fig. 6C) or decrease in viability (Fig. 6D) were observed in the presence of COH29, indicating COH29 exhibits antitumor activity without causing genotoxicity.

Molecular Pharmacology Fast Forward. Published on March 26, 2015 as DOI: 10.1124/mol.114.094987
This article has not been copyedited and formatted. The final version may differ from this version.

DISCUSSION

In this study we sought to further define the biological effects of the novel RNR inhibitor COH29, which effectively inhibits proliferation of various cancer cell lines, especially ovarian cancer and leukemic cells, and overcomes resistance to the RNR inhibitor hydroxyurea (Zhou et al. 2013). Building upon our initial observation that the BRCA1 deficient ovarian cancer cell line UWB1.289 was particularly sensitive to COH29 we determined BRCA1 status itself could account for this effect. Reconstitution of BRCA1 activity in the HCC1937 human breast cancer cell line, which expresses a truncated, inactive BRCA1 protein,(Tomlinson et al. 1998) in the stable transfectant clone HCC1937-BRCA1 blunted response to COH29 *in vitro* and *in vivo*. In addition, siRNA knockdown of BRCA1 increased sensitivity to COH29 in A2780 (BRCA1 wt) cells. As shown in Supplemental Figure 1, 72 h treatment with COH29 resulted in lower survival in A2780 cells transfected with BRCA1 siRNA than those transfected with control siRNA. These data suggested BRCA1 deficiency exaggerates the antiproliferative effect of COH29 treatment.

The signaling initiated by DNA damage is initially mediated by 'ataxia-telangiectasia-mutated' (ATM) and 'ATM and Rad3-related (ATR) kinases. The Chk1 and Chk2 DNA-damage-response kinases lie downstream of ATM and ATR (Abbas et al. 2013). We observed that COH29 treatment led to more significant activation of ATM, Chk1, Chk2 and γH2AX in HCC1937 compared with HCC1937+BRCA1 cells. In addition, we found that γH2AX and phospho-ATM colocalize with foxo3 in the nucleus. These data indicate COH29 triggers ATM-foxo3-γH2AX complexes at sites of DNA damage.

Molecular Pharmacology Fast Forward. Published on March 26, 2015 as DOI: 10.1124/mol.114.094987
This article has not been copyedited and formatted. The final version may differ from this version.

As BRCA1 is a critical mediator of cellular response to DNA damage and of HR repair, (Moeller et al. 2009, Curtin 2012) this suggested that COH29 potency is modulated by the perturbed DNA repair pathways in BRCA1-deficient cells. Our observation that the GFP+ cell population was undetectable in HCC1937-DR-GFP cells suggested that HCC1937 cells are HR-deficient. When we investigated the effect of COH29 on the NHEJ repair pathway in HCC1937 cells using the EJ5-GFP reporter system we found that COH29 suppressed NHEJ repair efficiency (Fig. 5A). Our microarray analysis (Table 2) also provided preliminary data in support of this, although further experiments covering a time course, and validation of identified genes would be needed to draw a strong conclusion. This is the subject of ongoing investigation.

In response to DNA damage, Rad51 translocates from the cytosol to the nucleus to form nucleofilaments on ssDNA, which is an essential step to promote the HR repair pathway (Haaf et al. 1995, Baumann et al. 1996). By confocal microscopy, we observed that COH29 induced significantly more γH2AX foci in HCC1937 cells compared with HCC1937+BRCA1 cells. In contrast, COH29 induced Rad51 nuclear foci in HCC1937+BRCA1 cells (Fig. 5C), suggesting Rad51 has been recruited at damage sites to repair COH29-triggered DNA damage via the HR repair pathway in these BRCA1 wild-type cells. This effect of COH29 on Rad51 is similar to that documented for HU, which is known to stall replication forks (Petermann et al. 2010), with the important distinction that COH29 is 20-fold more potent than HU (Zhou et al. 2013), and is not appreciably genotoxic (Fig. 7). Taken together, these results suggested inhibition of the NHEJ repair pathway by COH29 could also contribute to COH29-induced DSBs in HR-deficient HCC1937 cells.

Molecular Pharmacology Fast Forward. Published on March 26, 2015 as DOI: 10.1124/mol.114.094987
This article has not been copyedited and formatted. The final version may differ from this version.

The NHEJ pathway is reported as the major pathway for DNA repair of radiation-induced DSBs in mammalian cells (Riballo et al. 2004). Furthermore, a previous report has also proposed that quiescent/slowly cycling CSCs (Cancer Stem Cells) are more likely to use the error prone NHEJ pathway, resulting in offspring with enhanced chemoresistance and metastatic abilities after replication (Maugeri-Sacca et al. 2012). This suggests that targeting the NHEJ pathway may be an effective way to kill cancer stem cells. Therefore, NHEJ inhibition may represent a potential strategy in patients with proficient NHEJ to increase the response to treatment.

However, the underlying mechanism of the effect of COH29 on DNA repair needs further evaluation. For instance, it is unclear whether this is a direct effect on the DNA repair machinery, or a consequence of depletion of dNTPs due to RNR inhibition. There are a handful of reports which indicate that other RNR inhibitors also affect DNA repair pathways and or checkpoints. As mentioned above, the prototypic RNR inhibitor HU, causes upregulation of Rad51, and formation of both Rad51 and γH2AX foci.(Petermann et al. 2010) Gemcitabine, a nucleoside analogue that also inhibits the RNR large subunit (Shao et al. 2006) has been shown to be more potent in BRCA1 deficient cells, synergize with cisplatin, and induce Rad51 and γH2AX foci. (Alli et al. 2011) Lin and colleagues knocked down RRM2 subunit expression and observed results consistent with what we see for COH29, which is a specific RRM2 inhibitor (Zhou et al. 2013); activation of Chk1, and upregulation of γH2AX. (Lin et al. 2011) The same group have recently shown that the RRM1 inhibitor Triapine (3-AP, 3-aminopyridine-2-carboxaldehyde thiosemicarbazone) caused Chk1 activation.(Lin et al. 2014).

Molecular Pharmacology Fast Forward. Published on March 26, 2015 as DOI: 10.1124/mol.114.094987
This article has not been copyedited and formatted. The final version may differ from this version.

Collectively, our data provide evidence that COH29 is an RNR inhibitor that can activate DNA damage checkpoints and suppress DNA repair functions without significant genotoxicity. In summary this report provides initial evidence that COH29 suppresses NHEJ repair, whether directly or indirectly, and that in the setting of HR deficiency – such as in BRCA1 mutants – this is a particularly effective approach *in vitro* and provides information to guide initial clinical development of this compound.

Molecular Pharmacology Fast Forward. Published on March 26, 2015 as DOI: 10.1124/mol.114.094987
This article has not been copyedited and formatted. The final version may differ from this version.

AUTHORSHIP CONTRIBUTIONS

Participated in Research Design: M-C Chen, Zhou, Zhang, Yuan, Un, Wu, Malkas, M. C-T Hu, Yen

Conducted Experiments: M-C Chen, Zhang, Yuan, S. Hu, Chou, C-H. Chen, Wu, Wang, Li, Su, Chung

Performed Data Analysis: M-C Chen, Zhou, Zhang, Yuan, Chou, C-H Chen, Wu, X Liu, Smith, Li, Warden, Z Liu, Su, Chung

Wrote or Contributed to the Writing of the Manuscript: M-C Chen, Un, Chou, C-H Chen, Wu, Smith, Warden, M. C-T. Hu, Yen

Molecular Pharmacology Fast Forward. Published on March 26, 2015 as DOI: 10.1124/mol.114.094987
This article has not been copyedited and formatted. The final version may differ from this version.

REFERENCES

Abbas, T, MA Keaton and A Dutta (2013). Genomic instability in cancer. *Cold Spring Harb Perspect Biol* **5**: **a012914**.

Alli, E, VB Sharma, AR Hartman, PS Lin, L McPherson and JM Ford (2011). Enhanced sensitivity to cisplatin and gemcitabine in Brca1-deficient murine mammary epithelial cells. *BMC Pharmacol* **11**: **7**.

Ashburner, M, CA Ball, JA Blake, D Botstein, H Butler, JM Cherry, AP Davis, K Dolinski, SS Dwight, JT Eppig, MA Harris, DP Hill, L Issel-Tarver, A Kasarskis, S Lewis, JC Matese, JE Richardson, M Ringwald, GM Rubin and G Sherlock (2000). Gene ontology: tool for the unification of biology. The Gene Ontology Consortium. *Nat Genet* **25**: **25-29**.

Baumann, P, FE Benson and SC West (1996). Human Rad51 protein promotes ATP-dependent homologous pairing and strand transfer reactions in vitro. *Cell* **87**: **757-766**.

Benjamini, Y and Y Hochberg (1995). Controlling the False Discovery Rate - a Practical and Powerful Approach to Multiple Testing. *Journal of the Royal Statistical Society Series B-Methodological* **57**: **289-300**.

Bennardo, N, A Cheng, N Huang and JM Stark (2008). Alternative-NHEJ is a mechanistically distinct pathway of mammalian chromosome break repair. *PLoS Genet* **4**: **e1000110**.

Chung, YM, SH Park, WB Tsai, SY Wang, MA Ikeda, JS Berek, DJ Chen and MC Hu (2012). FOXO3 signalling links ATM to the p53 apoptotic pathway following DNA damage. *Nat Commun* **3**: **1000**.

Curtin, NJ (2012). DNA repair dysregulation from cancer driver to therapeutic target. *Nat Rev Cancer* **12**: **801-817**.

DelloRusso, C, PL Welcsh, W Wang, RL Garcia, MC King and EM Swisher (2007). Functional characterization of a novel BRCA1-null ovarian cancer cell line in response to ionizing radiation. *Mol Cancer Res* **5**: **35-45**.

Deng, CX and SG Brodie (2000). Roles of BRCA1 and its interacting proteins. *Bioessays* **22**: **728-737**.

Gottipati, P, B Vischioni, N Schultz, J Solomons, HE Bryant, T Djureinovic, N Issaeva, K Sleeth, RA Sharma and T Helleday (2010). Poly(ADP-ribose) polymerase is hyperactivated in homologous recombination-defective cells. *Cancer Res* **70**: **5389-5398**.

Haaf, T, EI Golub, G Reddy, CM Radding and DC Ward (1995). Nuclear foci of mammalian Rad51 recombination protein in somatic cells after DNA damage and its localization in synaptonemal complexes. *Proc Natl Acad Sci U S A* **92**: **2298-2302**.

Hehlmann, R (2003). Current CML therapy: progress and dilemma. *Leukemia* **17**: **1010-1012**.

Helleday, T, E Petermann, C Lundin, B Hodgson and RA Sharma (2008). DNA repair pathways as targets for cancer therapy. *Nat Rev Cancer* **8**: **193-204**.

Hu, T, YM Chung, M Guan, M Ma, J Ma, JS Berek and MC Hu (2014). Reprogramming ovarian and breast cancer cells into non-cancerous cells by low-dose metformin or SN-38 through FOXO3 activation. *Sci Rep* **4**: **5810**.

Irizarry, RA, B Hobbs, F Collin, YD Beazer-Barclay, KJ Antonellis, U Scherf and TP Speed (2003). Exploration, normalization, and summaries of high density oligonucleotide array probe level data. *Biostatistics* **4**: **249-264**.

Keshelava, N, T Frgala, J Krejsa, O Kalous and CP Reynolds (2005). DIMSCAN: a microcomputer fluorescence-based cytotoxicity assay for preclinical testing of combination chemotherapy. *Methods Mol Med* **110**: **139-153**.

Lin, ZP, Y Lee, F Lin, MF Belcourt, P Li, JG Cory, PM Glazer and AC Sartorelli (2011). Reduced level of ribonucleotide reductase R2 subunits increases dependence on homologous recombination repair of cisplatin-induced DNA damage. *Mol Pharmacol* **80**: **1000-1012**.

Lin, ZP, ES Ratner, ME Whicker, Y Lee and AC Sartorelli (2014). Triapine disrupts CtIP-mediated homologous recombination repair and sensitizes ovarian cancer cells to PARP and topoisomerase inhibitors. *Mol Cancer Res* **12**: **381-393**.

Maugeri-Sacca, M, M Bartucci and R De Maria (2012). DNA damage repair pathways in cancer stem cells. *Mol Cancer Ther* **11**: **1627-1636**.

Miknyoczki, SJ, S Jones-Bolin, S Pritchard, K Hunter, H Zhao, W Wan, M Ator, R Bihovsky, R Hudkins, S Chatterjee, A Klein-Szanto, C Dionne and B Ruggeri (2003). Chemopotentiation of temozolomide, irinotecan, and cisplatin activity by CEP-6800, a poly(ADP-ribose) polymerase inhibitor. *Mol Cancer Ther* **2**: **371-382**.

Moeller, BJ, R Pasqualini and W Arap (2009). Targeting cancer-specific synthetic lethality in double-strand DNA break repair. *Cell Cycle* **8**: **1872-1876**.

Petermann, E, ML Orta, N Issaeva, N Schultz and T Helleday (2010). Hydroxyurea-stalled replication forks become progressively inactivated and require two different RAD51-mediated pathways for restart and repair. *Mol Cell* **37**: **492-502**.

Pierce, AJ, P Hu, M Han, N Ellis and M Jasin (2001). Ku DNA end-binding protein modulates homologous repair of double-strand breaks in mammalian cells. *Genes Dev* **15**: **3237-3242**.

Platt, OS (2008). Hydroxyurea for the treatment of sickle cell anemia. *N Engl J Med* **358**: **1362-1369**.

Reichard, P and A Ehrenberg (1983). Ribonucleotide reductase--a radical enzyme. *Science* **221**: **514-519**.

Riballo, E, M Kuhne, N Rief, A Doherty, GC Smith, MJ Recio, C Reis, K Dahm, A Fricke, A Krempler, AR Parker, SP Jackson, A Gennery, PA Jeggo and M Lobrich (2004). A pathway of double-strand break rejoining dependent upon ATM, Artemis, and proteins locating to gamma-H2AX foci. *Mol Cell* **16**: **715-724**.

Schneider, CA, WS Rasband and KW Eliceiri (2012). NIH Image to ImageJ: 25 years of image analysis. *Nat Methods* **9**: **671-675**.

Shao, J, B Zhou, B Chu and Y Yen (2006). Ribonucleotide reductase inhibitors and future drug design. *Curr Cancer Drug Targets* **6**: **409-431**.

Shao, J, B Zhou, L Zhu, W Qiu, YC Yuan, B Xi and Y Yen (2004). In vitro characterization of enzymatic properties and inhibition of the p53R2 subunit of human ribonucleotide reductase. *Cancer Res* **64**: **1-6**.

Shewach, DS and TS Lawrence (2007). Antimetabolite radiosensitizers. *J Clin Oncol* **25**: **4043-4050**.

Tomlinson, GE, TT Chen, VA Stastny, AK Virmani, MA Spillman, V Tonk, JL Blum, NR Schneider, Wistuba, II, JW Shay, JD Minna and AF Gazdar (1998). Characterization of a breast cancer cell line derived from a germ-line BRCA1 mutation carrier. *Cancer Res* **58**: **3237-3242**.

Un, F, C Qi, M Prosser, N Wang, B Zhou, C Bronner and Y Yen (2006). Modulating ICBP90 to suppress human ribonucleotide reductase M2 induction restores sensitivity to hydroxyurea cytotoxicity. *Anticancer Res* **26**: **2761-2767**.

Westerfield, M (1993). *The zebrafish book : a guide for the laboratory use of zebrafish (Brachydanio rerio)*. Eugene, OR, M. Westerfield.

Wooster, R and BL Weber (2003). Breast and ovarian cancer. *N Engl J Med* **348**: **2339-2347**.

Xue, L, B Zhou, X Liu, W Qiu, Z Jin and Y Yen (2003). Wild-type p53 regulates human ribonucleotide reductase by protein-protein interaction with p53R2 as well as hRRM2 subunits. *Cancer Res* **63**: **980-986**.

Young, CW and S Hodas (1964). Hydroxyurea: Inhibitory Effect on DNA Metabolism. *Science* **146**: **1172-1174**.

Zhou, B, L Su, S Hu, W Hu, ML Yip, J Wu, S Gaur, DL Smith, YC Yuan, TW Synold, D Horne and Y Yen (2013). A small-molecule blocking ribonucleotide reductase holoenzyme formation inhibits cancer cell growth and overcomes drug resistance. *Cancer Res* **73**: **6484-6493**.

Molecular Pharmacology Fast Forward. Published on March 26, 2015 as DOI: 10.1124/mol.114.094987
This article has not been copyedited and formatted. The final version may differ from this version.

FOOTNOTES

This research was supported by the National Cancer Institute of the National Institutes of Health grants [CA127541, CA113859, P30CA033572]; Taiwan Medical University grant [TMU102-AE1-B43]; and by the Avon Foundation for Women grant [02-2013-051]. The content is solely the responsibility of the authors and does not necessarily represent the official views of the National Institutes of Health.

Mei-Chuan Chen and Bingsen Zhou contributed equally to this work.

Affiliation for Yun Yen, MD, PhD for the duration of the work described herein: City of Hope National Medical Center, Department of Molecular Biology, 1500 E. Duarte Rd, Duarte, CA 91010.

Molecular Pharmacology Fast Forward. Published on March 26, 2015 as DOI: 10.1124/mol.114.094987
This article has not been copyedited and formatted. The final version may differ from this version.

LEGENDS FOR FIGURES

Figure 1. BRCA1 status affects COH29 cytotoxicity in ovarian cancer cells. (A) Dose response curves for ovarian cancer cells expressing wt BRCA1 (OV90) or mutant BRCA1 (UWB1.289) incubated with COH29 for 72 h. **(B)** Dose-dependent effects of COH29 on cell viability in UWB1.289 and UWB1.289+BRCA1 cells. Cell viability was assessed by MTS assay. UWB1.289+BRCA1 is a stable cell line derived from BRCA1-null UWB1.289 described in Materials and Methods. The points depicted represent an average of three independent experiments with error bars indicated.

Figure 2. BRCA1 status affects COH29 antitumor activity in breast cancer cells. (A) Cell viability of COH29 in HCC1937 and HCC1937+BRCA1 cells assessed by MTS assay, and growth of tumor explants established with HCC1937 **(B)** and HCC1937+BRCA1 **(C)** cells in the mammary fat pads of female NSG mice. Mice were treated daily with 400 mg/kg COH29 or vehicle as indicated. Results are the mean ± standard error of tumor measurements from 4 mice/group.

Figure 3. COH-29 treatment activates DNA damage checkpoint. (A) The effect of COH29 treatment on DNA damage checkpoint proteins in HCC1937 and HCC1937+BRCA1 human breast cancer cells assessed by Western Blot. **(B)** The effect of HU (Hydroxyurea) on DDR-associated proteins was assessed by Western blot analysis. Cells were treated with COH29 at the indicated doses for 24 h and cell lysates were subjected to immunoblotting using the indicated antibodies.

Molecular Pharmacology Fast Forward. Published on March 26, 2015 as DOI: 10.1124/mol.114.094987
This article has not been copyedited and formatted. The final version may differ from this version.

Figure 4. Effect of COH29 on Colocalization of DDR-related proteins. (A) The effect of COH29 on DDR-associated proteins was assessed in cytoplasm and nucleus by Western blot analysis. Cells were treated with COH29 at the indicated doses for 24 h and cell lysates were subjected to immunoblotting using the indicated antibodies. FOXO3 activity is indicated by the levels of its downstream target p27Kip1. GAPDH and lamin A/C represent the fractionation and loading controls of cytosolic(C) and nuclear(N) extracts. **(B)** Phospho-ATM, γH2AX, and together with foxo3 in the nucleus was assessed by indirect immunofluorescence assay.

Figure 5. Effect of COH29 on DNA repair, and expression of DSB markers. Flow cytometric analysis of **(A)** HCC1937- EJ5GFP and **(B)** HCC1937+BRCA1-DRGFP cells treated with 0, 0.25 and 0.5 of the IC_{50} concentration of COH29, with the normalized percentage of GFP-positive cells shown to the right. * $p < 0.05$, compared with COH-29 untreated cells. **(C)** The effect of COH29 on RAD51 and γ-H2AX foci was assessed by immunofluorescence assay described in Materials and Methods.

Figure 6. Effect of COH29 compared to HU in zebrafish genotoxicity assay. A. Wild-type zebrafish embryos at 4 dpf exposed to HU as indicated. Morphological changes in the eye and heart development are indicated by the arrowheads. **B.** Bar graph of the effect (mutant embryos) of a series of different concentrations of HU on zebrafish (0, 0.5, 1, 5, 10, 20, 50 mM, n = 50, performed in triplicate). **C.** Wild-type zebrafish embryos at 4 dpf exposed to COH29 as indicated. Bar = 100 μm. **D**. Bar graph

Molecular Pharmacology Fast Forward. Published on March 26, 2015 as DOI: 10.1124/mol.114.094987
This article has not been copyedited and formatted. The final version may differ from this version.

of the effect (survival embryos) of a series of different concentrations of COH29 on zebrafish (0, 10, 20, 50, 100 μM, n = 46, performed in triplicate).

Molecular Pharmacology Fast Forward. Published on March 26, 2015 as DOI: 10.1124/mol.114.094987
This article has not been copyedited and formatted. The final version may differ from this version.

TABLES

Table 1. Comparison of the Effect of COH29 in several cell lines

BRCA1	Cell Line	IC_{50} of COH29 (μM)
wild-type	OV90	31.57 ± 3.35
mutant	UWB1.289	12.30 ± 1.25
	UWB1.289/BRCA1	23.52 ± 2.38
mutant	HCC1937	7.25 ± 0.64
	HCC1937/BRCA1	35.01 ± 3.63

Molecular Pharmacology Fast Forward. Published on March 26, 2015 as DOI: 10.1124/mol.114.094987
This article has not been copyedited and formatted. The final version may differ from this version.

Table 2. Gene Ontology Enrichment of Genes Downregulated by COH29 Treatment

Comparison	COH29 effect in BRCA1-deficient cells	COH29 effect in BRCA1 wt cells	BRCA1 wt vs BRCA1 deficient cells
Treatment groups	HCC1937-COH29 vs HC1937	HCC1937BRCA1-COH29 vs HC1937BRCA1	HCC1937+BRCA1-COH29 vs HCC1937-COH29
DNA repair, *P*-value	0.018	1.6×10^{-5}	0.001
DNA ligation involved in DNA repair, *P*-value	0.00065	0.0066	0.06
Double-strand break repair via nonhomologous end joining, *P*-value	0.049	0.041	0.04
Double-strand break repair via homologous recombination, *P*-value	0.0069	0.0046	0.26
Double-strand break repair, *P*-value	0.0015	6.9×10^{-5}	0.3

Fig. 1

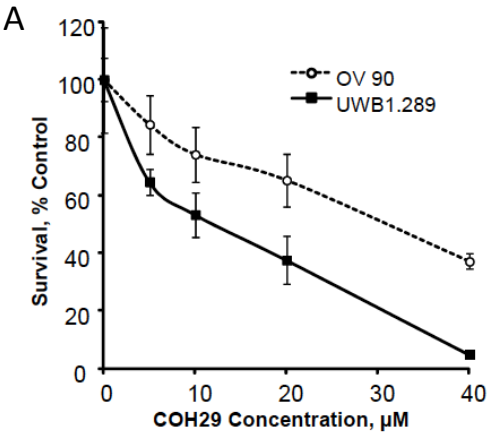
A
120
100
80
60
40
20
0
Survival, % Control
OV 90
UWB1.289
0
10
20
30
40
COH29 Concentration, μM

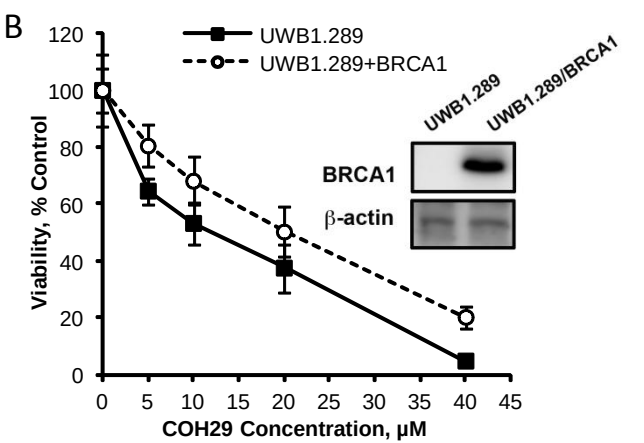
B
120
100
80
60
40
20
0
Viability, % Control
UWB1.289
UWB1.289+BRCA1
UWB1.289
UWB1.289/BRCA1
BRCA1
β-actin
0
5
10
15
20
25
30
35
40
45
COH29 Concentration, μM

Fig. 2

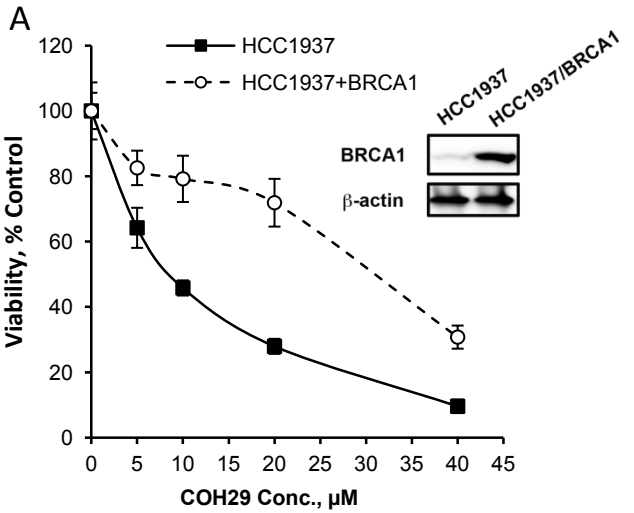
A
HCC1937
HCC1937+BRCA1
HCC1937
HCC1937/BRCA1
BRCA1
β-actin
Viability, % Control
COH29 Conc., μM

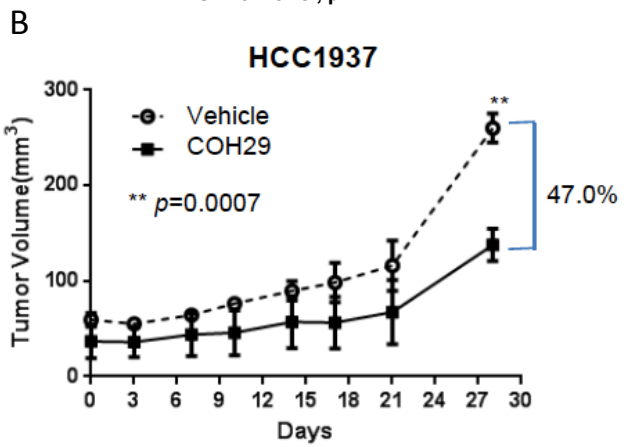
B
HCC1937
Vehicle
COH29
** p=0.0007
47.0%
Tumor Volume(mm3)
Days

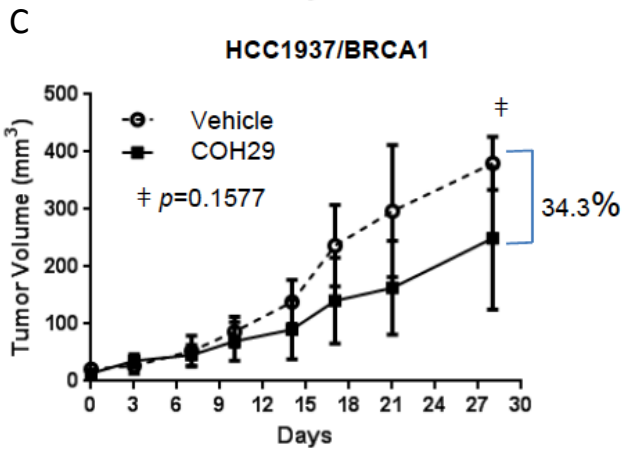
C
HCC1937/BRCA1
Vehicle
COH29
‡ p=0.1577
34.3%
Tumor Volume (mm3)
Days

Fig. 3

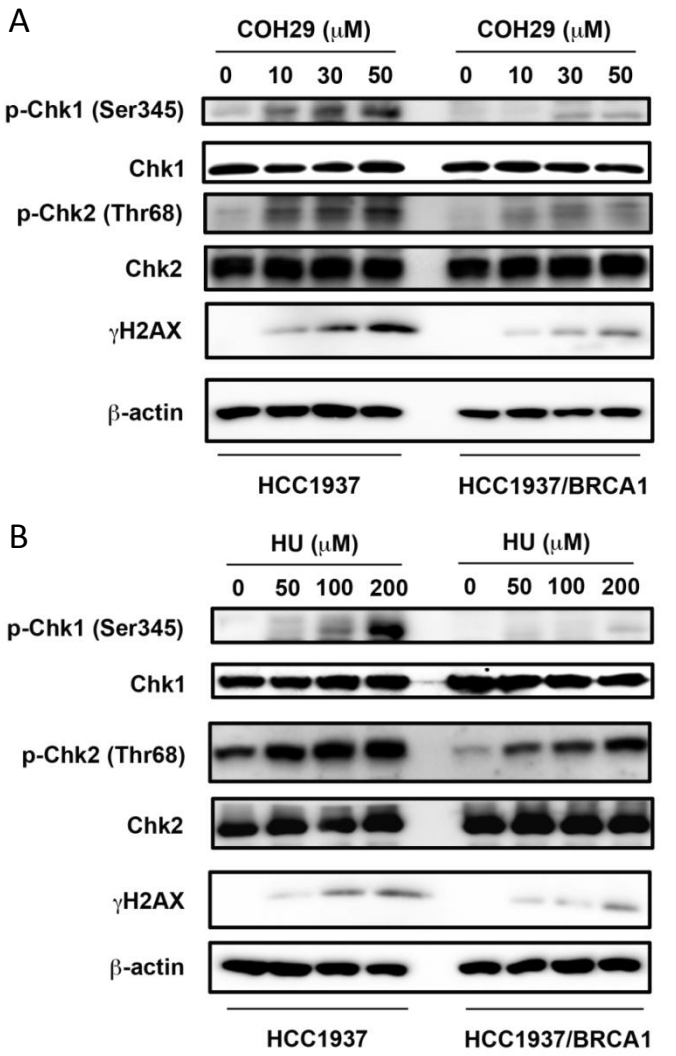
A
COH29 (μM)
0 10 30 50
COH29 (μM)
0 10 30 50
p-Chk1 (Ser345)
Chk1
p-Chk2 (Thr68)
Chk2
γH2AX
β-actin
HCC1937
HCC1937/BRCA1
B
HU (μM)
0 50 100 200
HU (μM)
0 50 100 200
p-Chk1 (Ser345)
Chk1
p-Chk2 (Thr68)
Chk2
γH2AX
β-actin
HCC1937
HCC1937/BRCA1

Fig. 4

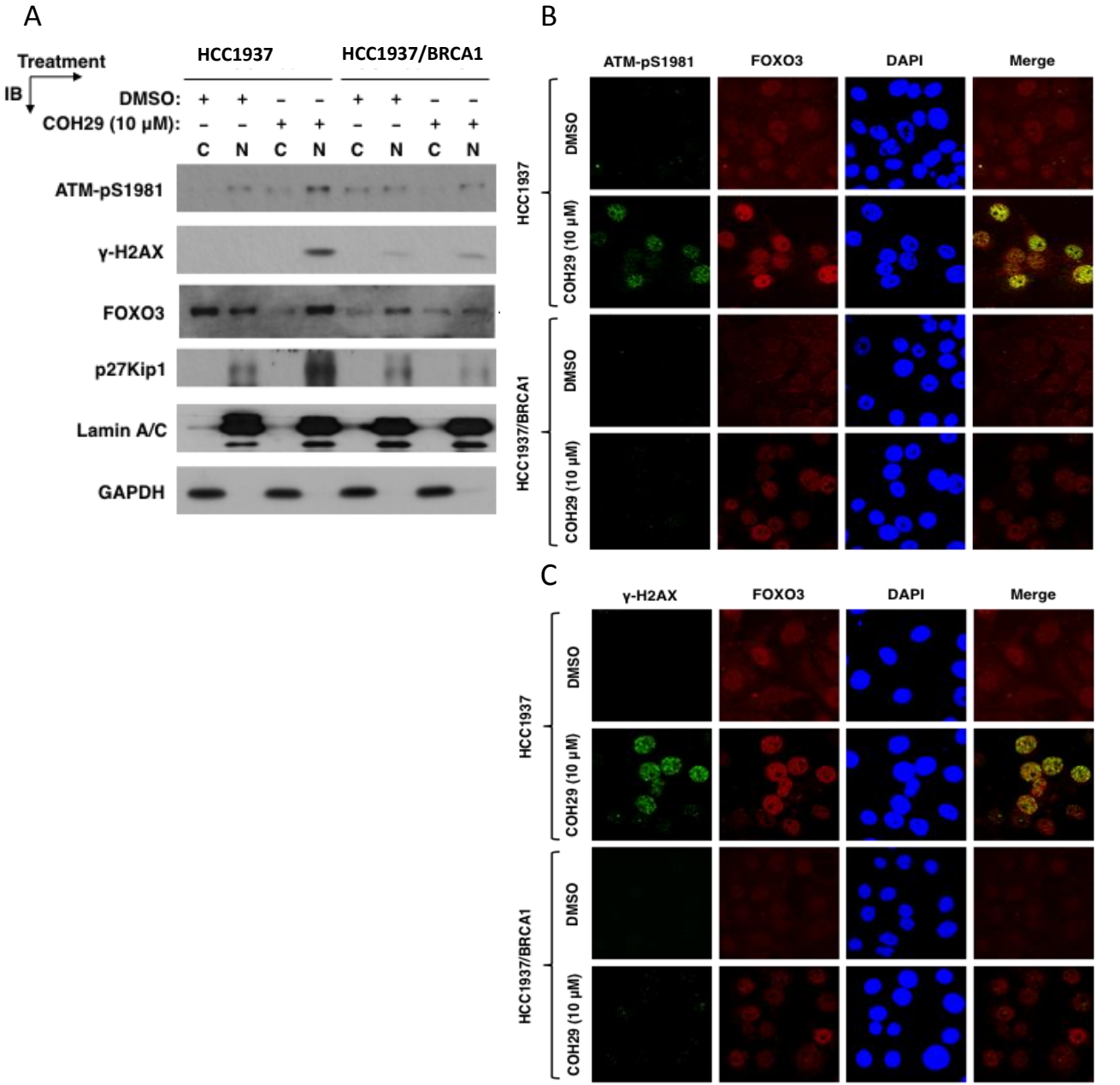
A
Treatment
IB
HCC1937
HCC1937/BRCA1
DMSO:
COH29 (10 μM):
C N C N C N C N
ATM-pS1981
γ-H2AX
FOXO3
p27Kip1
Lamin A/C
GAPDH
B
ATM-pS1981
FOXO3
DAPI
Merge
HCC1937
HCC1937/BRCA1
DMSO
COH29 (10 μM)
C
γ-H2AX
FOXO3
DAPI
Merge
HCC1937
HCC1937/BRCA1
DMSO
COH29 (10 μM)

Fig. 5

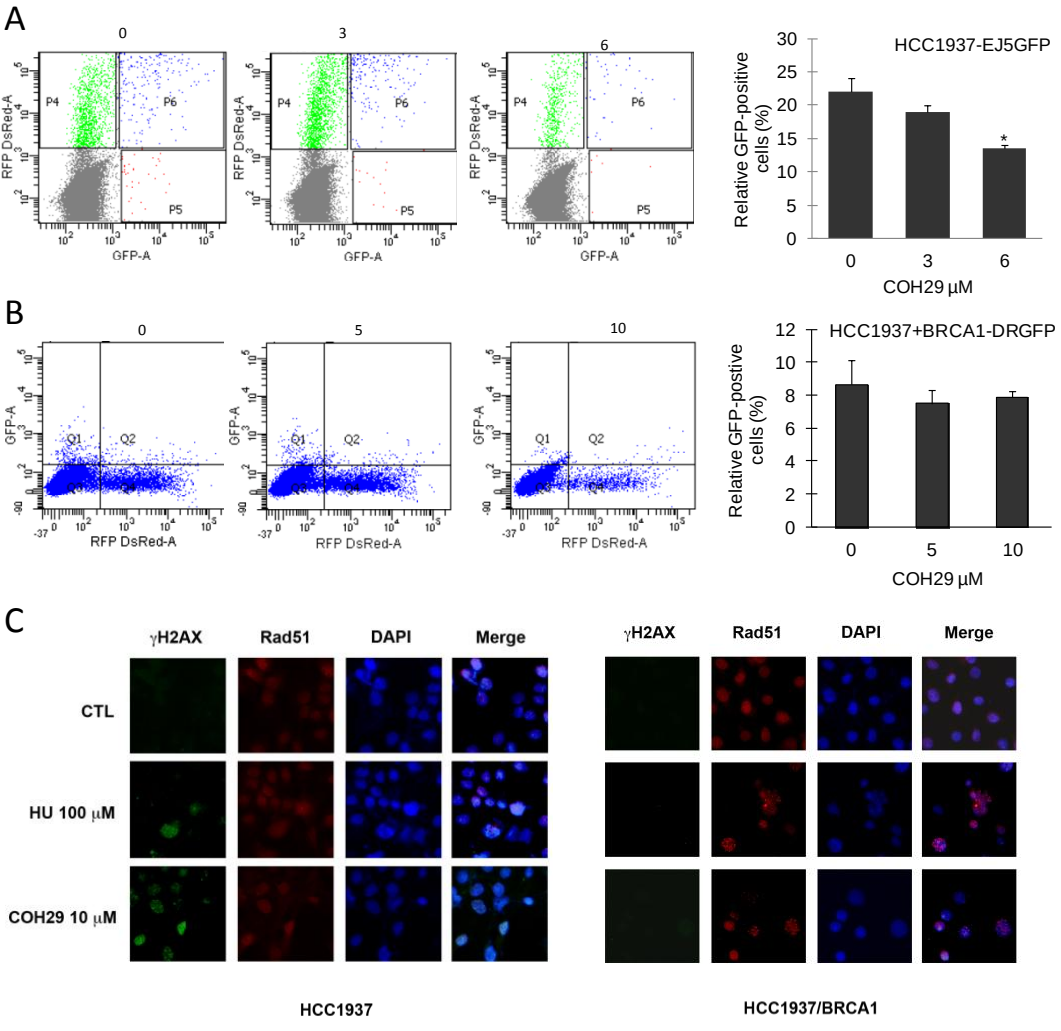
A
0
3
6
P4
P6
P5
RFP DsRed-A
GFP-A
HCC1937-EJ5GFP
Relative GFP-positive cells (%)
COH29 μM
B
5
10
Q1
Q2
HCC1937+BRCA1-DRGFP
C
γH2AX
Rad51
DAPI
Merge
CTL
HU 100 μM
COH29 10 μM
HCC1937
HCC1937/BRCA1

Fig. 6

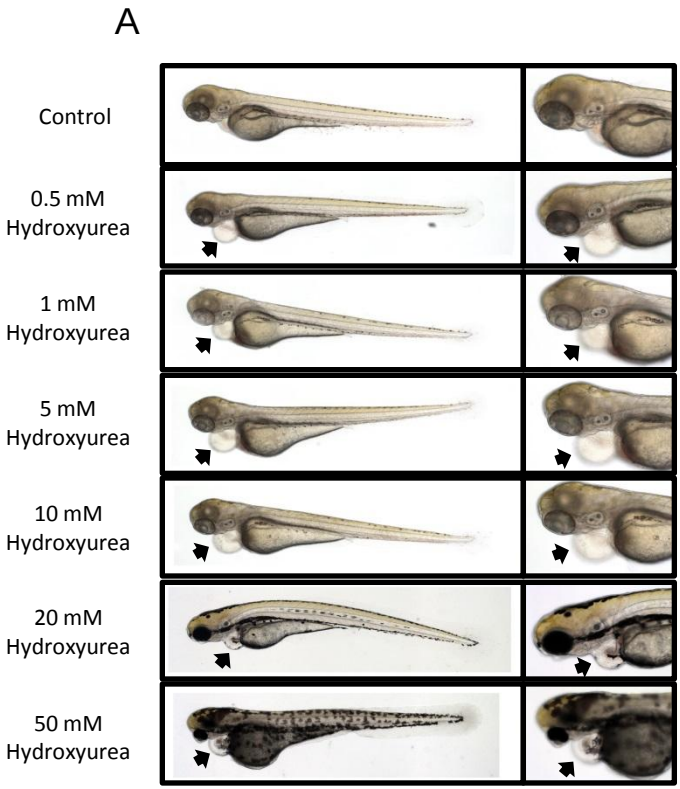
A
Control
0.5 mM Hydroxyurea
1 mM Hydroxyurea
5 mM Hydroxyurea
10 mM Hydroxyurea
20 mM Hydroxyurea
50 mM Hydroxyurea

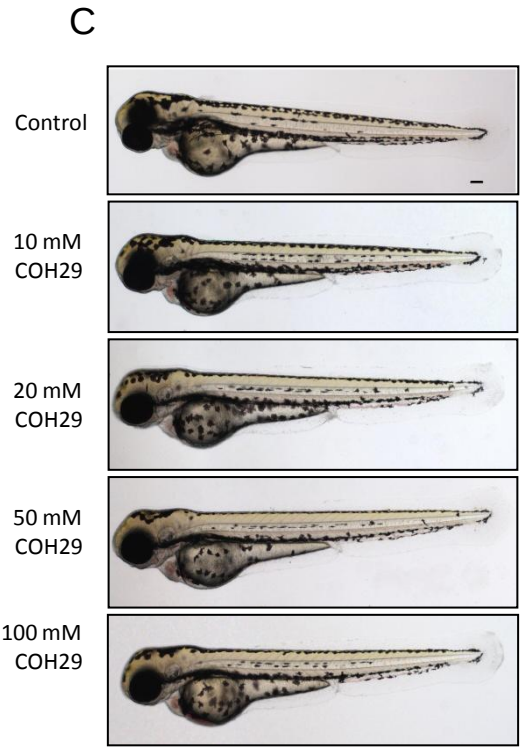
C
Control
10 mM COH29
20 mM COH29
50 mM COH29
100 mM COH29

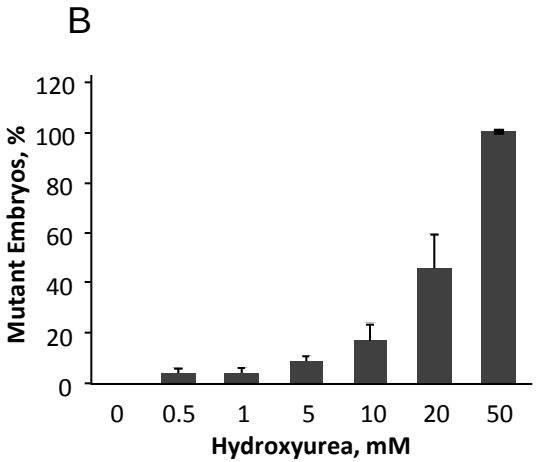
B
Mutant Embryos, %
120
100
80
60
40
20
0
0
0.5
1
5
10
20
50
Hydroxyurea, mM

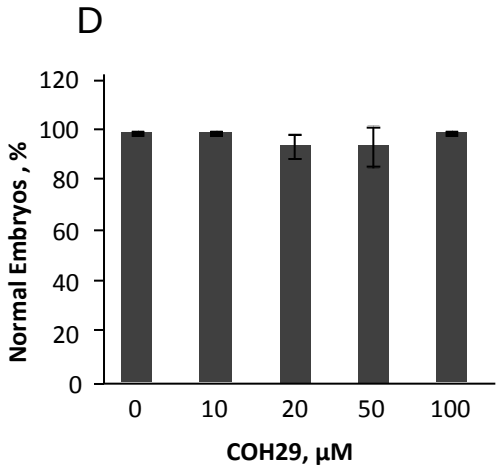
D
Normal Embryos , %
120
100
80
60
40
20
0
0
10
20
50
100
COH29, µM